Bioelectromagnetics 20:194–201 (1999)

Kinetics of Sealing for Transient Electropores in Isolated Mammalian Skeletal Muscle Cells

Martin Bier,* Stephanie M. Hammer, Daniel J. Canaday, and Raphael C. Lee*

The Department of Organismal Biology and Anatomy, The Department of Surgery, Pritzker School of Medicine, The University of Chicago, Chicago, Illinois

Permeabilization of the plasma membrane by electrical forces (electroporation) can be either transient or stable. Although the exact molecular mechanics have not yet been described, electroporation is believed to initiate primarily in the lipid bilayer. To better understand the kinetics of membrane permeabilization, we sought to determine the time constants for spontaneous transient pore sealing. By using isolated rat *flexor digitorum brevis* skeletal muscle cells and a two-compartment diffusion model, we found that pore sealing times (τ_P) after transient electroporation were approximately 9 min. τ_P was not significantly dependent on the imposed transmembrane potential. We also determined the transmembrane potential (ΔV_m) thresholds necessary for transient and stable electroporation in the skeletal muscle cells. ΔV_ms ranging between 340 mV and 480 mV caused a transient influx of magnesium, indicating the existence of spontaneously sealing pores. An imposed ΔV_m of 540 mV or greater led to complete equilibration of the intracellular and extracellular magnesium concentrations. This finding suggests that stable pores are created by the larger imposed transmembrane potentials. These results may be useful for understanding nerve and skeletal muscle injury after an electrical shock and for developing optimal strategies for accomplishing transient electroporation, particularly for gene transfection and cell transformation. Bioelectromagnetics 20:194–201, 1999.

Key words: electroporation; pore sealing; sealing kinetics

INTRODUCTION

The integrity of the plasma membrane is vital to cell survival. For mammalian cells, one of the most important functions of the membrane is to maintain transmembrane ionic gradients and cytoplasmic electrolyte homeostasis. At physiologic temperatures, the hydrophobic interior of the lipid bilayer membrane forms a barrier that is highly impermeable to hydrophilic molecules. The movement of an ion from aqueous media through an intact membrane can require energy levels as high as ~60 kcal/mole [Parsegian, 1975], which is two orders of magnitude larger than thermal energy at physiologic temperatures.

There are several common medical disorders associated with altered cell membrane structure and plasma membranes that are permeable to extracellular solutes. Electrical shock trauma, mechanical crush, and hyperthermia can lead to rhabdomyolysis and the release of intracellular contents from the cytoplasm into the circulation [Lee and Kolodney, 1987; Lee et al., 1988, 1992; Odeh, 1992]. Exposure to ionizing radiation and post-ischemic tissue reperfusion can produce superoxide free radicals, which react with and permeabilize the lipid bilayer [Freeman and Crapo, 1982; Odeh, 1992]. Under these conditions, cell survival depends on how rapidly the membrane spontaneously seals. It is therefore essential, when developing therapeutic strategies, to understand the probability and kinetics of spontaneously sealing damaged membranes.

Contract grant sponsor: Electric Power Research Institute; Contract grant sponsor: Empire State Electric Energy Research Corporation; Contract grant sponsor: individual electric utilities that include Niagara Mohawk Power Corp., Northeast Utilities Service Co., Public Service Electric & Gas Co., Public Service Co. of Oklahoma, and Wisconsin Electric Power Company.

*Correspondence to: Martin Bier and Raphael C. Lee, Section of Plastic and Reconstructive Surgery, Department of Surgery, MC 6035, University of Chicago, 5841 S. Maryland Ave., Chicago, IL 60637. E-mail: mbier@surgery.bsd.uchicago.edu

Received for review 12 April 1997; Final revision received 13 August 1998

A widely used model for the study of membrane permeabilization is electroporation. Biological membranes undergo transient or permanent increased permeability after exposure to brief electric field pulses with field strengths exceeding a certain threshold value [Neumann and Rosenheck, 1972; Benz et al., 1979; Teissie and Tsong, 1981; Escaunde-Geraud, 1988; Lee and Kolodney, 1987; Hibino et al., 1991; Lee et al., 1993]. In studies of gene transfer and cell transformation, electroporation is now used routinely to conveniently permeabilize membranes and introduce macromolecules into various cell types [Benz and Zimmerman, 1980; Neumann et al., 1982; Rols and Teissie, 1990; Tsong, 1990a; Potter, 1992; Potter and Cooke, 1992]. Partly because of its reproducibility, there is growing interest in the exact molecular mechanics of electroporation.

Cell membrane electropermeabilization is considered transient when electropores spontaneously seal and stable when electropores do not seal. The imposed transmembrane potentials (ΔV_m) and duration thresholds required to generate transient or stable pores differ [Kinosita and Tsong, 1977; Benz et al., 1979; Weaver and Powell, 1989; Lee et al., 1993]. If electropores accumulate in the membrane after multiple shocks, they may coalesce into even larger defects [Teissie and Tsong, 1981; Bhatt et al., 1990], which can lead to cell lysis. It is important to characterize the dynamics of the membrane pores that are formed by electroporation to understand the molecular mechanisms of membrane electropermeabilization.

In this study, we used a reliable method of electroporation to permeabilize cell membranes and examine the kinetics of transient electroporation and plasma membrane damage. A magnesium-sensitive fluorescent probe was used to precisely quantify ion flux after electroporation. We determined the thresholds of induced ΔV_ms necessary to create transient and stable electropores in the skeletal muscle cell membrane. By using a two-compartment diffusion model, we calculated the time constant of transient pore lifetimes (τ_P) after electroporation by using a range of electric field strengths. This insight into the kinetics of electropore formation and closure furthers our understanding of the mechanics of electropermeabilization, and may be useful for developing therapeutic models for disorders that result from damaged cell membranes.

MATERIALS AND METHODS

High-voltage electrical contacts cause extensive damage to skeletal muscle and nerve cells, resulting in tissue necrosis, and often lead to high amputation rates [Lee and Kolodney, 1987; Zachary et al., 1990]. Because skeletal muscle cells are relatively large and therefore experience significant damage in electrical injury accidents, these cells were selected for study. Relatively weak electric field strengths can be used to permeabilize skeletal cell membranes, an important advantage because the use of smaller electric fields helps eliminate the complicating effects of Joule heating.

Cell Preparation

Flexor digitorum brevis skeletal muscle cells from 4-week-old female Sprague-Dawley rats were harvested. Individual cells were separated by incubation at 37 °C for 2.5 h with continuous agitation in a solution of 0.3% type II collagenase (Worthington, Freehold, NJ) in phosphate-buffered saline (PBS) containing calcium and the pH buffer *N*-2-hydroxyethylpiperazine-*N'*-2-ethanesulfonic acid (HEPES, Gibco, Grand Island, NY). After separation, the cells were washed and then isolated by a brief, gentle trituration. The cells were maintained in porous Transwell dishes (Costar, Cambridge, MA) for 48 h at 37 °C in Dulbecco's minimum essential media (Gibco), supplemented with 25 mM HEPES (Gibco), 10% horse serum (Gibco), 100 U/ml penicillin, and 100 μg/ml streptomycin. Viability of the cells was checked by subjecting a subset of the cells to the carboxyfluorescein diacetate viability test [Freeman and Crapo, 1982] and by visual inspection for normal striations.

Cells were incubated at 37 °C in 5 μM Mag-Fura-2 AM (Molecular Probes, Eugene, OR) to load the ratiometric magnesium sensitive dye into the cytoplasm. The cells were then washed and incubated in calcium-free PBS for 75 min at 37 °C to allow full hydrolysis of the dye by esterases within the cell.

Cells were loaded by pipette into a custom optical chamber designed to create a uniform electric field in the media. The chamber was fabricated by machining a 1-cm-wide square well in a circular 0.5-inch-thick polysulfonate block. The polysulfonate is electrically insulating. The bottom of the well was formed by mounting a 180-micron rectangular glass coverslip into a recess surrounding the well. On one pair of opposite walls, 1-cm-wide platinum electrodes were mounted. They were bathed in PBS (electrical conductivity 0.4 Siemens/cm) without calcium to dissociate excitation-contraction coupling. Then 10 mM [Mg^{2+}] was added to the solution to replace the extracellular calcium and to produce a magnesium gradient across the cell membrane. The divalent cation Mg^{2+} stabilizes the cell membrane in a manner similar to the membrane stabilization by the divalent cation Ca^{2+}. The solution also contained 50 mM HEPES to buffer alkaline changes caused by electrochemical reactions at the electrodes. To characterize the thermal transients in the PBS solution caused by Joule heating, a small fast thermistor was mounted on the chamber. The thermistor was positioned in the PBS solution. A series

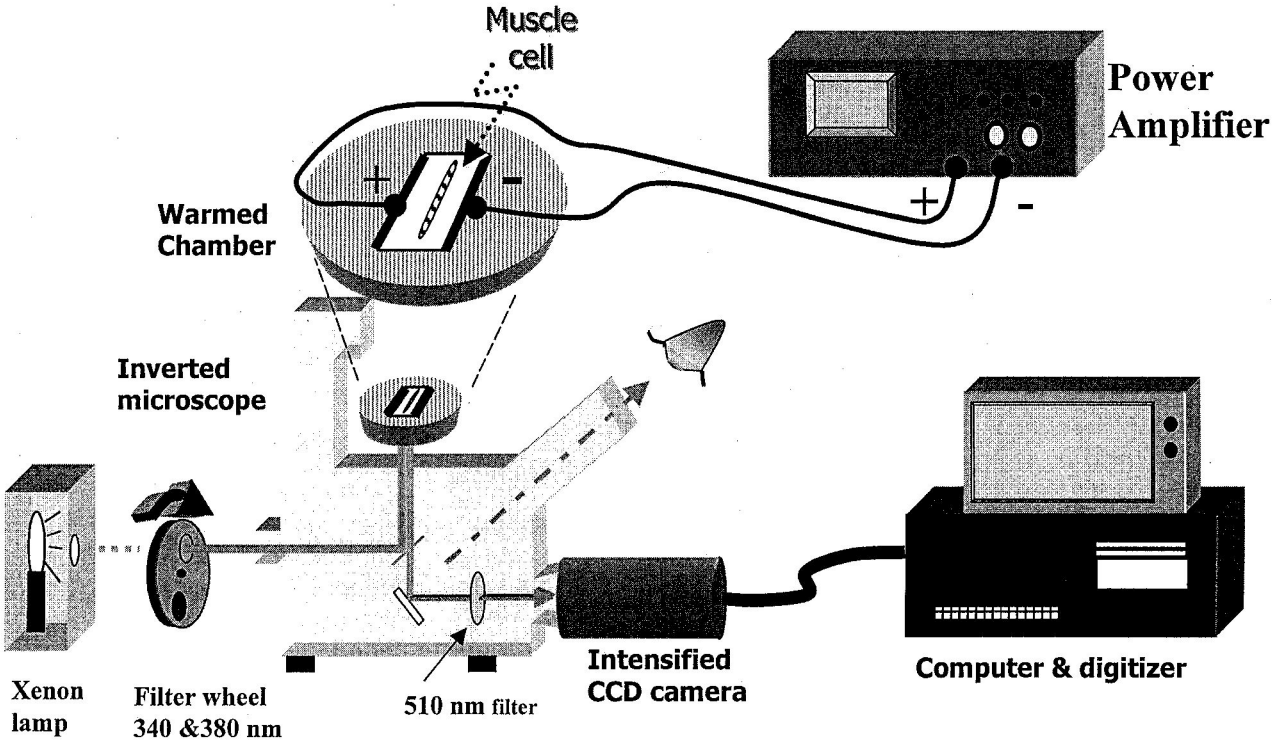

Fig. 1. Experimental apparatus for two-dimensional video fluorometry for intracellular [Mg^{2+}] studies. The computer controlled filter switches between 340-nm and 380-nm excitation filters. An isolated myocyte is located in a custom optical chamber. Field pulses are applied by using a pulse generator and power supply connected to platinum electrodes located at opposite ends of the custom optical chamber.

of tests was performed in which 4-ms current pulses were applied over the range actually used in the electroporation experiments. The temperature was calculated from the thermistor calibration data.

Video Microscopy

Ratiometric video fluorometry was used to obtain 2-dimensional data regarding magnesium flux. The custom optical chamber was mounted on a Nikon inverted microscope equipped with fluorescent optics (Fig. 1). The Mag-Fura-2 dye was excited by using a xenon arc lamp filtered alternately at λ_{ex} = 340 nm and λ_{ex} = 380 nm by using a computer-controlled filter changer (AZI, Avon, MA). The emission fluorescence was filtered at λ_{em} = 510 nm and then intensified, digitized, and monitored by using a video-image intensifier and CCD camera (VideoScope, Washington, D.C.) attached to a video-digitizing board (Universal Imaging, West Chester, PA). Ion concentrations were determined by calculating the emission ratio of dye at 340 nm and 380 nm. This ratio is a qualitative representation of the ion concentration because the dye displays a spectral excitation shift upon chelation with magnesium ions. The ratio can be numerically calibrated by using standardized magnesium solutions according to equations by Grynkiewicz et al. [1985]. The ratio images of Mag-Fura-2 emission were digitized and stored in a personal computer for analysis. The ratio images were displayed by the computer as pseudocolor images (Fig. 2). It is important to note that using a ratiometric fluorescent emission technique allows accurate measurement in this type of experiment. Despite the possible dye leaking through by electroporation, changes in intensity occur proportionately at both measured wavelengths. This ratio provides a stable ion concentration/spectral emission relationship.

Cell Exposure

Each cell was placed by pipette into the custom designed microscopy chamber and oriented with its long axis perpendicular to the applied electric field. We used skeletal muscle cells of 50 to 60 μm in diameter. The perpendicular alignment caused the maximal ΔV to be imposed over a greater fraction of the cell surface (Fig. 3). The effect of membrane changes can be more accurately measured with perpendicular orientation because the rate of magnesium diffusion into the cytoplasm after membrane permeabilization is proportional to the total surface area affected.

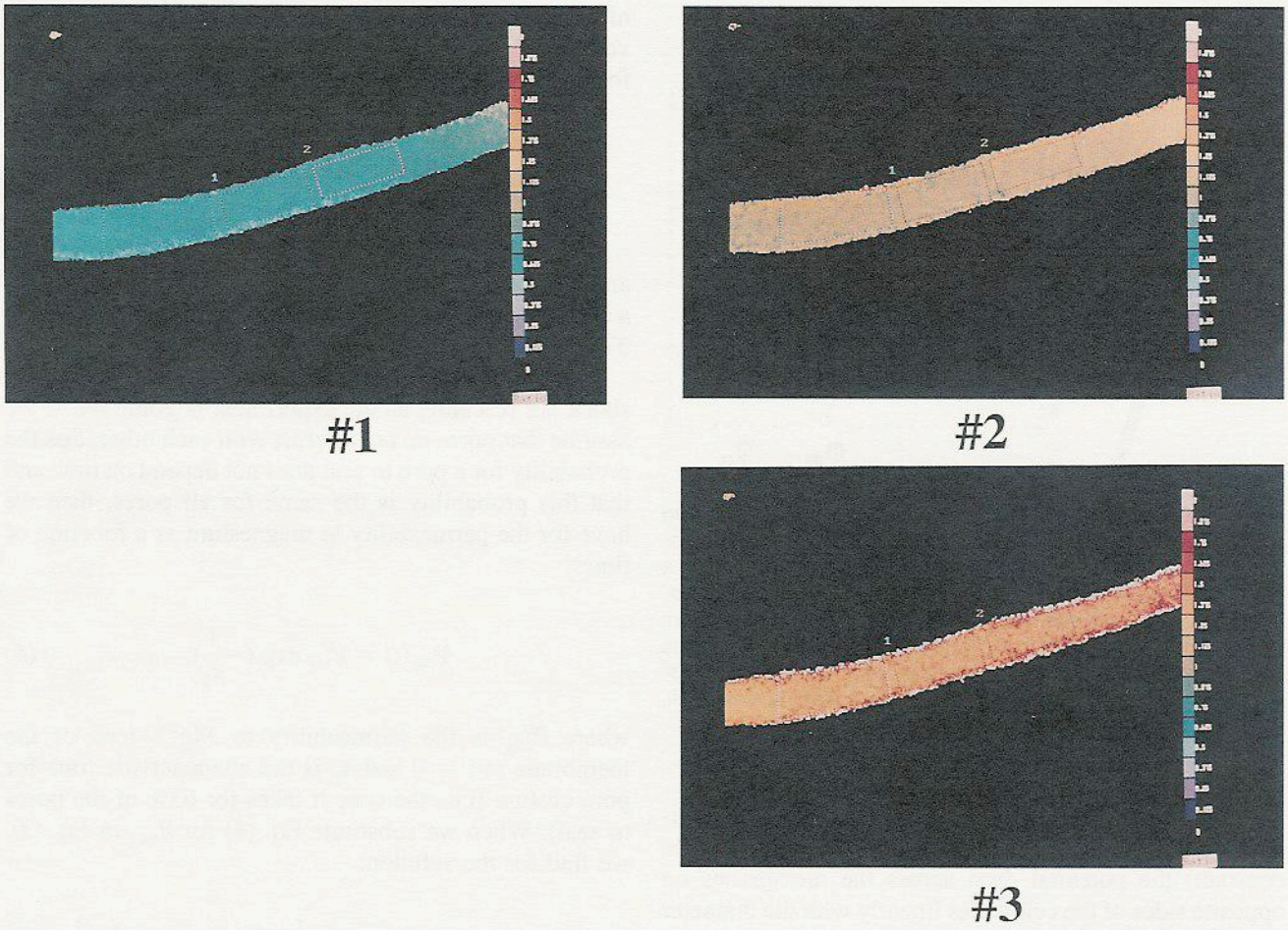

Fig. 2. Pseudocolor magnesium ion concentration image of skeletal muscle cell by using Mag-Fura-2 dye. The shock was applied between images 1 and 2. The sequence represents the magnesium ion influx attributable to the increased membrane permeability.

Single 4-ms field pulses to bring about bath field strengths of about 150 V/cm were delivered. This requires currents in the range of 0.1 to 1.0 Ampere. This results in transmembrane potentials in the cells from ~340 mV to ~600 mV. The electrodes were placed 1 cm apart at opposite ends of the exposure chamber. The pulses corresponded to the root-mean-square duration of a sinusoidal wave half-cycle of the commercial 60 Hz power lines and were short enough to avoid significant Joule heating effects. Tests with multiple shocks of ΔV_m~600 mV separated by 20 min caused a transient solution temperature rise with a peak value of less than 0.5 °C, low enough to avoid any pathologic changes caused by heat. The cells were monitored for changes in magnesium concentrations to determine ion flux across the plasma membrane.

The sensitivity of the fluorometric magnesium assay to membrane ionic permeability was verified by chemically permeabilizing the cell membrane by using the detergent sodium dodecyl sulfate (SDS, 0.08%). Contact with this detergent produces large defects in the lipid bilayers of cell membranes. The cells were treated identically to those used in electroporation experiments described before, except that an aliquot of a 1.0% SDS solution was added instead of applying an electrical shock. The resulting change in cytoplasmic magnesium was recorded.

Data Analysis

Skeletal muscle cells are characteristically elongated and cylindrical in shape. In humans, their length ranges from 0.1 to 100 mm and their diameter ranges from 50 to 500 μm. The electrical properties of mammalian skeletal muscle cell membranes have been well characterized [Schanne et al., 1978].

The magnitude of ΔV is a function of the dimensions of the cell and the membrane space constant λ_m, which reflects the conductivity of the membrane relative

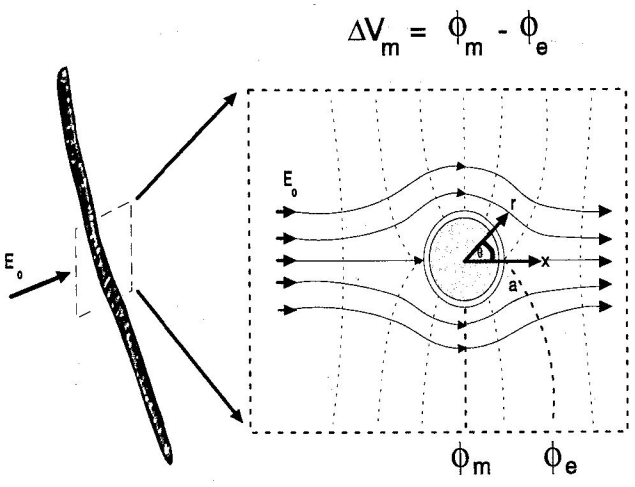

Fig. 3. (Left) An isolated myocyte with electric field (E_o) applied perpendicularly. (Right) A close-up view of the idealized myocyte with a perfectly insulating membrane. E_o is applied in the x direction. The dependence of the imposed transmembrane potential (ΔV_m) on skeletal muscle cell orientation in the uniform electric field (E_o) is graphically illustrated for the cell. Φ_m is the potential midway through the cell, and Φ_e is the electrical potential located along the isopotential curve at the end of the cell. ΔV_m is described by Eq. (1).

to the intracellular and extracellular fluid. For an electrically small cell (meaning with length less than its space constant) the potential drop across the membranes on opposite sides of the cell varies linearly with the diameter of the cell [Gaylor et al., 1988]. The induced transmembrane potential can then be estimated from the externally applied field E_o as:

$$\Delta V = \frac{3}{2} E_0 \, r \cos(\theta), \tag{1}$$

where r is the radius of the cell and θ is relative to the direction of E_o (Fig. 3).

Changes in the cell membrane permeability manifest themselves as a influx of magnesium ions into the cell. The inflow of magnesium into the cell equals:

$$\Phi_{Mg} = AP_{Mg}[C_0 - C_i(t)], \tag{2}$$

where P_{Mg} represents the permeability of the membrane to magnesium, A is the total cell membrane area, and C_0 and C_i represent the magnesium concentration outside and inside the cell, respectively. In our experiment, C_0 is the magnesium concentration in the bath and, because the volume of the bath is many orders of magnitude larger than the volume of the cell, it can be taken to be constant. The inflow of magnesium also equals the increase of the amount of magnesium inside the cell. The total amount of magnesium inside the cell is $VC_i(t)$, where V is the volume of the cell. We find, thus, a differential equation for $C_i(t)$ as a function time:

$$V\frac{d}{dt}C_i(t) = AP_{Mg}[C_0 - C_i(t)]. \tag{3}$$

In many applications, P is constant and this leads to an exponential relaxation of $C_i(t)$ to the value of C_0 with a characteristic time (the time for C_0 - $C_i(t)$ to decrease to 37% of the original value) of $t = V/(P_{Mg} A)$.

In our case, the pores that were formed during the shock are resealing as the experiment is going on. If we assume that pores do not interact with each other, that the probability for a pore to seal does not depend on time and that this probability is the same for all pores, then we have for the permeability to magnesium as a function of time:

$$P_{Mg}(t) = P^0_{Mg} \exp\left(-\frac{t}{\tau_p}\right), \tag{4}$$

where P^0_{Mg} is the permeability to Mg^{2+} ions of the membrane at $t = 0$ and τ_p is the characteristic time for pore closure (i.e., the time it takes for 63% of the pores to seal). When we substitute Eq. (4) for P_{Mg} in Eq. (3), we find for the solution:

$$C_i(t) = C_0 - (C_0 - C_i(0)) \exp\left[-\frac{\tau_p}{\tau_L}\left[1 - \exp\left(-\frac{t}{\tau_p}\right)\right]\right], \tag{5}$$

where $C_i(0)$ is the intracellular magnesium concentration at $t = 0$ and $\tau_L = V/(P^0_{Mg} A)$, i.e., the relaxation time for the intracellular magnesium concentration if no pore sealing were to take place.

When we perform a Taylor expansion of Eq. (5) at $t = 0$ we find for the constant and the linear term:

$$C_i(t) \approx C_i(0) + \frac{C_0 - C_i(0)}{\tau_L} t. \tag{6}$$

This formula should give a good description of the apparently linear increase of $C_i(t)$ right after electroporation.

Numerical Analysis

We fitted the measured postshock electroporation intracellular Mg^{2+} concentration to a curve like Eq. (5) and a least squares criterion was used to find the values for τ_L and τ_P that lead to the best fit. Figure 4 shows the datapoints and fitted curves. All datapoints were given the same weight. For all experiments, an

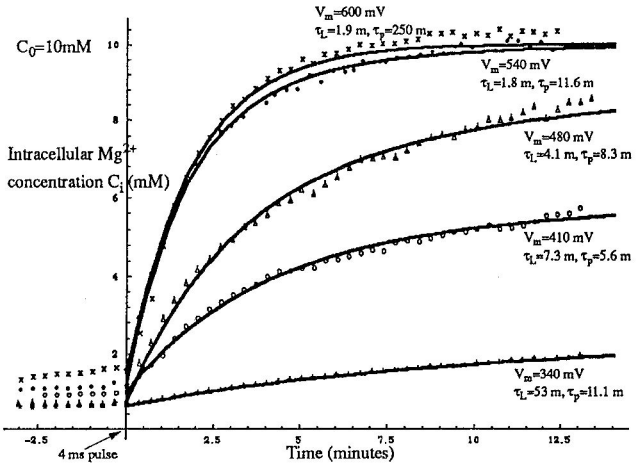

Fig. 4. Effects of imposed transmembrane potentials (ΔV_m) on isolated myocyte intracellular [Mg^{2+}]. τ_L and τ_p are derived from Eq. (5). τ_L is inversely proportional to the membrane permeability, P^0_{Mg}, immediately after the shock. τ_p is the time constant of transient pore lifetimes after spontaneously reversible electroporation. It appears that P^0_{Mg} goes up with the voltage of the shock. τ_p appears to be independent of that voltage until a certain threshold is reached beyond which pores do not seal any longer.

average of the preshock cytoplasmic [Mg^{2+}] was taken to determine $C_i(0)$.

RESULTS

Studies done to establish the accuracy of the model were encouraging. Resting intracellular magnesium concentration was monitored up to 1 h and remained stable in controls. The resting concentration was 0.86 ± 0.01 mM (n = 9), a value similar to published values [Alvarez-Leefmans et al., 1986]. As noted, chemically induced cell membrane permeabilization by SDS caused a rapid influx of extracellular magnesium, which was detected and quantified by using the probe. As will be discussed, high-intensity imposed transmembrane voltages brought about an equilibration of extra- and intracellular ion concentrations, as would be expected after a large, stable increase in membrane permeability.

Response to Electroporation

Figure 4 shows the experimental data as well as the optimal fits of Eq. (5). The two characteristic times, τ_L and τ_p, that lead to the best fit are indicated with each curve. τ_L is proportional to $1/P^0_{Mg}$ and a geometrical factor that does not change much from cell to cell. P^0_{Mg} is the permeability immediately after the shock and as such is a measure for the damage caused by the shock. The data show that P^0_{Mg} increases by a factor 30 when the shock voltage, ΔV_m, increases from 340 to 540 mV. The pore sealing time, τ_p, is observed to be independent of ΔV_m up to a threshold at around 600 mV. The average τ_p is about 9 min. Pores appear to be stable (i.e., τ_p becomes very large) after a shock of sufficiently high voltage. It has been postulated [Litster, 1975] that pores that are larger than a certain critical size will not seal, but instead experience a force toward further expansion. It is conceivable that for sufficiently large ΔV_m many such big, stable pores are being formed.

When, in Eq. (5), t becomes very large, $C_i(t)$ asymptotically approaches $C_0 - (C_0 - C_i(0)) \exp[-\tau_p/\tau_L]$. Considering this limit and the data we can distinguish three regimes. (1) For sufficiently small shocks (<340 mV), $\tau_p/\tau_L = \tau_p P^0_{Mg} A/V$ will be close to zero because of a small P^0_{Mg}. This results in an $\exp[-\tau_p/\tau_L]$ that is so close to one that $C_i(t)$ will not discernibly rise above $C_i(0)$ after the shock. (2) For shocks between 340 mV and 480 mV, the value of $\exp[\tau_p/\tau_L]$ is such that the intracellular Mg^{2+} concentration relaxes to a value between C_0 and $C_i(0)$. (3) For ΔV_ms larger than ~540 mV, the value of $\exp[-\tau_p/\tau_L]$ is close to zero and $C_i(t)$ appears to relax to the extracellular Mg^{2+} concentration. It is also in agreement with the theory, cf. Eq. (6), that we get a faster relaxation to the asymptotic value for larger ΔV_ms.

Electropore Longevity

Several tests were performed to determine whether sealing occurred up to 1 h after electroporation. In these experiments, the extracellular magnesium concentration was doubled at various times after shock. At 45 min after shock, the addition of magnesium to the solution after shocks of ΔV_ms ranging from 340 mV to 480 mV had little or no effect on the intracellular magnesium concentration, apart from the expected flux caused by an equilibrium shift across the membrane. This indicated that the membrane electropores had spontaneously sealed and remained sealed. After imposed ΔV_ms of 540 mV and 600 mV, the addition of magnesium to the bath solution up to 60 min after shock caused a step increase in $C_i(t)$, verifying the presence of stable pores at these imposed voltages. The imposed ΔV_ms necessary for pore formation are similar to those found in other studies using different cell lines, such as those used for genetic transfection [Benz and Zimmerman, 1980; Rols and Teissie, 1990; Tsong, 1990a].

DISCUSSION

It is appropriate here to discuss the effects of cell orientation to the applied electric field. We know that we can estimate the imposed transmembrane potential from Eq. (1). For any given applied electric field E_o, those areas of the cell perfectly perpendicular to E_o will be

exposed to a maximal imposed voltage (ΔV_{max}), whereas other areas of the cell will be exposed to ΔV_m (Fig. 3). For a given electric field strength, this may result in some areas of the cell incurring more damage than other areas. The inflow of Mg^{2+} into the cell right after the shock is a result of the cumulative damage. If there are many transient pores, the presence of a few stable pores will not be noticeable in the timespan covered in Figure 4, especially when already the transient electroporation suffices to bring about an almost complete equilibration. This explains why for 540 mV we find a "transient" value of τ_p in cells that appear to still have stable pores 60 min after shock.

The integrity of the cell membrane is essential for biochemical regulation of cellular processes and ultimately for cell survival itself. Electropermeabilization is a convenient and relevant method for the study of cell membrane damage. In this study, we have examined the ability of the cell to maintain transmembrane ionic gradients under imposed extracellular fields that mimic the conditions in the human upper extremity during high-voltage (1–20 kV) electrical shock. Such high voltage exposures generally last only 10 to 100 ms because the victim is blown away from the source by the thermoacoustic blast that ensues from the sudden release of energy. Also, strong currents cause general muscle contraction that propels the victim away. In these accidents, the total release of energy is usually not sufficient to raise the temperature in the tissue significantly and lead to any thermal damage [Tropea and Lee, 1992]. Our results suggest that the electric field in tissues within the upper extremity of the typical victim of high-voltage electrical shock [Lee et al., 1993] is large enough to permeabilize the skeletal muscle cell membrane to mobile ions. Most important, our study provides a model by which we can better understand the molecular mechanics of membrane behavior after electropermeabilization.

The major purpose of this study was to characterize the kinetics of transient pore sealing in mammalian cell membranes. The results of extensive modeling have been reported for the characteristics of aqueous pores in lipid bilayer membranes and the effects of pores on the permeability and stability of the membrane [Neumann and Rosenheck, 1972; Benz and Zimmerman, 1980; Teissie and Tsong, 1981; Powell et al., 1986; Powell and Weaver, 1986; Tsong, 1996; Weaver and Chizmadzhev, 1996]. A wide range of sealing times after reversible electrical breakdown in lipid bilayers has been noted [Teissie and Tsong, 1981; Weaver and Powell, 1989; Tsong, 1990a,b, 1996]. Experimental data on the sealing characteristics of pores created by electroporation have not yet been sufficiently examined. Erythrocytes and their ghosts have frequently been the subject of electroporation studies [Butler and Grant, 1977; Zachary et al., 1990; Hibino et al., 1991; Tsong, 1996]. Erythrocyte membranes are specialized and, therefore, not generally representative of cell membranes, although they are obviously important. Saulis et al. (1991) described the kinetics of pore sealing in human red blood cells after electroporation. They found that the restoration of membrane barrier function to medium-sized molecules (i.e., ascorbic acid and mannitol) occurred more quickly (2–3 min) than complete sealing against smaller molecules such as sodium ions (10–15 min).

The differences between the geometries of skeletal muscle cells and erythrocytes result in different transmembrane potentials being imposed for a given electric field. The skeletal muscle plasma membrane may be a more appropriate model for studying membrane damage. In this study, we have examined the ability of the skeletal muscle cell membrane to maintain its barrier to a divalent cation. We determined the thresholds of electroporation on skeletal muscle cells and examined the time constants of transient pore lifetimes. Membrane damage was field-strength dependent. No observable cell membrane damage was incurred after imposed potentials of less than 340 mV.

The results of this study indicate the formation of two populations of membrane defects, transient and stable, depending on the conditions of electric field exposure. It appears that transient pores began to form when the imposed transmembrane potential (ΔV_m) exceeded 300 to 350 mV. We found that the restoration of the cell membrane barrier to cationic flux occurred in ~9 min. The characteristic pore lifetimes (sealing times) did not appear to be voltage-dependent. When ΔV_ms exceeding ~600 mV were delivered, stable pores dominate the equilibration kinetics.

This study is an attempt to further our understanding of the dynamics of cell membrane damage and sealing. Understanding the kinetics of transient pore lifetimes in mammalian skeletal muscle cells is essential for developing a numerical model that may aid many applications that involve understanding of cell membrane repair dynamics, including gene transfection, cell translocation, and electrically mediated tissue injury studies.

ACKNOWLEDGMENTS

The authors gratefully acknowledge the editorial assistance of Diane Rudall, Tatiana Tkachenko, and Mary Favazza.

REFERENCES

Alvarez-Leefmans FJ, Gamino SM, Giraldez F, Gonzalez-Serratos H. 1986. Intracellular free magnesium in frog skeletal muscle fibers

measured with ion-selective micro-electrodes. J Physiol Lond 378: 461–483.

Benz R, Zimmerman U. 1980. Relaxation studies on cell membranes and lipid bilayers in the high electric field range. Bioelectrochem Bioenerg 7:723–739.

Benz R, Beckers F, Zimmermann U. 1979. Reversible electrical breakdown of lipid bilayer membranes: a charge-pulse relaxation study. J Membr Biol 48:181–204.

Bhatt DL, Gaylor DC, Lee RC. 1990. Rhabdomyolysis due to pulsed electric fields. Plast Reconstr Surg 86:1–3.

Butler ED, Grant TD. 1977. Electrical injuries with special reference to the upper extremities. Am J Surg 134:95–99.

Escaunde-Geraud ML, Rols MP, DuPont MA, Gas N, Teissie J. 1988. Reversible plasma membrane ultrastructural changes correlated with electropermeabilization in Chinese hamster ovary cells. Biochim Biophys Acta 939:247–259.

Freeman BA, Crapo JD. 1982. Biology of disease: free radicals and tissue injury. Lab Invest 47:412–442.

Gaylor DC, Prakah-Asante K, Lee RC. 1988. Significance of cell size and tissue structure in electrical trauma. J Theor Biol 133:223–237.

Grynkiewicz G, Poenie M, Tsien R. 1985. A new generation of Ca^{2+} indicators with greatly improved fluorescence properties. J Biol Chem 260:3440–3450.

Hibino M, Shigemori M, Itoh H, Nagayama K, Kinosita K. 1991. Membrane conductance of an electroporated cell analyzed by submicrosecond imaging of transmembrane potential. Biophys J 59:209–220.

Kinosita K, Tsong TY. 1977. Formation and resealing of pores of controlled sizes in human erythrocyte membrane. Nature 268:438–441.

Lee RC, Kolodney MS. 1987. Mechanisms of electrical trauma: electrical breakdown of cell membranes. Plast Reconstr Surg 80:672–679.

Lee RC, Gaylor DC, Bhatt DL, Israel DA. 1988. Role of cell membrane rupture in the pathogenesis of electrical trauma. J Surg Res 44: 709–719.

Lee RC, River LP, Pan F-S, Li J, Wollmann RL. 1992. Surfactant-induced sealing of electropermeabilized skeletal muscle membranes in vivo. Proc Natl Acad Sci USA 89:4524–4528.

Lee RC, Canaday DJ, Hammer SM. 1993. Transient and stable ionic permeabilization of isolated skeletal muscle cells following electrical shock. Am J Burn Care Rehabil 14:528–540.

Litster JD. 1975. Stability of lipid bilayers and red blood cell membranes. Phys Lett 53A:193–194.

Neumann E, Rosenheck K. 1972. Permeability changes induced by electric impulses in vesicular membranes. J Membr Biol 10:279–290.

Neumann E, Schaefer-Ridder M, Wang Y, Hofschneider PH. 1982. Gene transfer into mouse lyoma cells by electroporation in high electric fields. EMBO J 1:841–845.

Odeh M. 1992. The role of reperfusion-induced injury in the pathogenesis of the crush syndrome. In: Epstein F, editor. Mechanisms of disease. N Engl J Med 324:1417–1422.

Parsegian VA. 1975. Ion-membrane interactions as structural forces. Ann NY Acad Sci 264:161–174.

Potter H. 1992. Protocols for using electroporation to stably or transiently transfect mammalian cells. In: Chang DC, Chassy BM, Saunders JA, Sowers AE, editors. Guide to electroporation and electrofusion. San Diego: Academic Press. p. 457–464.

Potter H, Cooke SWF. 1992. Gene transfer into adherent cells growing on microbeads. In: Chang DC, Chassy BM, Saunders JA, Sowers AE, editors. Guide to electroporation and electrofusion. San Diego: Academic Press. p. 201–208.

Powell KT, Weaver JC. 1986. Transient aqueous pores in bilayer membranes: a statistical theory. Bioelectrochem Bioenerg 15:211–227.

Powell KT, Derrick EG, Weaver JC. 1986. A quantitative theory of reversible electrical breakdown in bilayer membranes. Bioelectrochem Bioenerg 15:243–255.

Rols MP, Teissie J. 1990. Electropermeabilization of mammalian cells: quantitative analysis of the phenomenon. Biophys J 58:1089–1098.

Saulis G, Venslauskas MS, Naktinis J. 1991. Kinetics of pore resealing in cell membranes after electroporation. Bioelectrochem Bioenerg 26:1–13.

Schanne O, Ruiz P, Ceretti E. 1978. Impedance measurements in biological cells. New York: Wiley.

Teissie J, Tsong TY. 1981. Electric field induced transient pores in phospholipid bilayer vesicles. Biochemistry 20:1548–1554.

Tropea BI, Lee RC. 1992. Thermal injury kinetics in electrical trauma. J Biomech Engr 114:241–250.

Tsong TY. 1990a. Electroporation of cell membranes. Biophys J 60:297–306.

Tsong TY. 1990b. On electroporation of cell membranes and some related phenomena. Bioelectrochem Bioenerg 24:271–295.

Tsong TY. 1996. Electrically stimulated membrane breakdown. In: Lynch PT, Davey MR, editors. Electrical manipulation of cells. London: Chapman and Hall.

Weaver JC, Chizmadzhev YuA. 1996. Theory of electroporation: a review. Bioelectrochem Bioenerg 41:135–160.

Weaver JC, Powell KT. 1989. Theory of electroporation. In: Neumann E, Sowers A, Jordan C, editors. Electroporation and electrofusion in cell biology. New York: Plenum Press.

Zachary LM, Lee RC, Gottlieb LJ. 1990. Evolving clinical and scientific concepts of upper extremity electrical trauma. Hand Clin 6:243–252.

Zimmermann U, Pilwat G, Riemann F. 1975. Preparation of erythrocyte ghosts by dielectric breakdown of the cell membrane. Biochim Biophys Acta 375:209–219.